International Journal of Modelling and Simulation

ISSN: 0228-6203 (Print) 1925-7082 (Online) Journal homepage: www.tandfonline.com/journals/tjms20

An MHD nanofluid flow with Marangoni laminar boundary layer over a porous medium with heat and mass transfer

T. Anusha, L. M. Pérez, U. S. Mahabaleshwar & D. Zeidan

To cite this article: T. Anusha, L. M. Pérez, U. S. Mahabaleshwar & D. Zeidan (2026) An MHD nanofluid flow with Marangoni laminar boundary layer over a porous medium with heat and mass transfer, International Journal of Modelling and Simulation, 46:2, 366-382, DOI: 10.1080/02286203.2024.2335112

To link to this article: https://doi.org/10.1080/02286203.2024.2335112

Published online: 04 Apr 2024.

INTERNATIONAL JOURNAL OF MODELLING AND SIMULATION
2026, VOL. 46, NO. 2, 366–382
https://doi.org/10.1080/02286203.2024.2335112

An MHD nanofluid flow with Marangoni laminar boundary layer over a porous medium with heat and mass transfer

T. Anusha[a], L. M. Pérez[b], U. S. Mahabaleshwar[a] and D. Zeidan[c]

[a]Department of Studies in Mathematics, Davangere University, Davangere, India; [b]Departamento de Física, FACI, Universidad de Tarapacá, Arica, Chile; [c]School of Electrical Engineering and Information Technology, German Jordanian University, Amman, Jordan

ABSTRACT

The current work considers two-dimensional incompressible fluid flow with heat transfer over a porous medium with mass transpiration and Marangoni boundary condition. The nanoparticles of graphene are mixed in water to improve thermal efficiency. It behaves as a heater upon increasing its solid volume fraction, Eckert number, and as a cooler upon increasing suction. This flow has remarkable interest due to its applications in glues, silicon wafers, heat exchangers, paints, crystal growth in space, etc. The ordinary differential equations (ODEs) are obtained from the considered partial differential equations (PDEs) using similarity transformation technique. Then the solutions are analytically recovered from the system of ODEs. The solutions of temperature and concentration fields are obtained in terms of Laguerre polynomial. The impacts of different parameters, such as Marangoni number, inverse Darcy number, Prandtl number, and Eckert number are analysed using graphical observations. Specially mentioned is Marangoni convection, which contains many industrial and engineering applications such as in nanotechnology, atomic reactors, soap films, semiconductor processing, and atomic reactors. This work adds the effect of graphene water nanofluid which enhance the thermal efficiency in a better way than the base fluid and explains the physical problem on the basis of chemically radiative Marangoni flow.

ARTICLE HISTORY

Received 14 February 2023
Accepted 22 March 2024

KEYWORDS

Brinkman ratio; Eckert number; graphene; Marangoni number; porous media; radiations

1. Introduction

Nanofluid (NF) refers to a well-blended mixture of nanoparticles in a base fluid that effectively cools systems operating in a high temperature range and has numerous thermal uses. Due to the development of the Lorentz force, the introduction of the magnetohydrodynamic (MHD) force will have a greater impact on the flow. MHD flow is crucial to the manufacturing of petroleum products and metallurgical operations. It should be noted that the final product formed depends on how quickly these processes cool. Several solutions for MHD flow with slip were discovered by Turkyilmazoglu [1]. Recent instances of MHD unstable stagnation point flow engineering applications were explored by Fang et al. [2]. The stresses brought on by a transverse gradient of surface tension acting at the interfaces in industrial processes dealing with liquid-liquid and gas-liquid interfaces result in fluid motions known as Marangoni convection. These interfaces induce convection because of buoyancy and Marangoni stresses, even in the absence of applied velocities or external momentum sources like pressure gradients. The thermosolutal Marangoni boundary layer, which forms at the liquid-liquid and gas-liquid interfaces, is dissipative in nature, and it plays a crucial role in many real-world applications, including metallurgy, semiconductor manufacturing, crystal formation, and space materials. Thus, in order to get the desired result, it is required to investigate the interactions between the relevant forces caused by pressure gradients, surface tension gradients, temperature gradients, and viscous dissipation at the interfaces between heat and mass transmission. Many industrial processes, including device heat exchange and cooling of engines can greatly benefit from solving stretching sheet difficulties. Many scholars are interested in the stretching sheet difficulties as a result [2,3]. The MHD flow caused by stretching and shrinking sheets is, respectively, examined by Hamad [4] and Fang and Zhang [5]. Mahabaleshwar [6,7] thoroughly investigated the stretching and convection issues. Additionally, the flow in porous media has various industrial and engineering applications. It can be found in some natural things, like limestone and human lungs, in thermal energy storage, in solar power collectors, and in electrochemical and chemical

CONTACT D. Zeidan dia.zeidan@gju.edu.jo School of Electrical Engineering and Information Technology, German Jordanian University, Amman, Jordan

catalytic reactors. Recently, a lot of work has been done on the flow due to porous media [8–11]. Zao et al. [12,13], Merkin et al. [14], and Mahabaleshwar et al. [15] worked on the Darcy-Brinkman model. Rohni et al. [16] studied mixed convective flow over porous media with temperature slip, and Khan et al. [17] worked on mixed convective radiative flow with convex and concave effects. Yacob et al. [18] studied the convective boundary conditions in the NF.

When changes in surface tension gradients occur in heat and mass or in both gradients, the Marangoni effect is produced in the fluid flow. This effect is widely utilized in welding, crystal growth, soap stabilisation, and so on. The current model has important uses in the fabrication of hydrophilic surfaces like silicon wafers, welding and metallurgical processes, investigations on crystal growth, geosciences, and space technologies. In addition, thermosolutal Marangoni convection has important uses in the metallurgical and semiconductor industries, where its importance may be seen in the control of heat and mass transport in metallic fluids. Arifin et al. [19] provided a comprehensive explanation of this Marangoni effect idea. The Italian scientist Carlo Giuseppe Matteo Marangoni first identified this Marangoni effect in the 1860s while examining how oil drops spread on a water surface. He attributed this pattern to local variations in interfacial tension, which are the macroscopic expression of a liquid flow. See other references on the Marangoni effect in [20–22].

Motivated by all previous works, the current work examines that two-dimensional incompressible flow over a porous medium with the Marangoni boundary condition by adding graphene nanoparticles in order to increase the thermal properties (see Choi and Eastman [23]). The yielded solution is in the form of an exponential and a Laguerre polynomial. The behavior of the solution is analysed using various parameters such as the Marangoni and inverse Darcy numbers, the Brinkman ratio, the Prandtl number, and the Eckert number. The structure of the current paper is as follows: Section 2 identifies the physical model. Section 3 presents the solution to the model equations. Results and discussion of the current investigations are provided in Section 4. Finally, Section 5 describes conclusions and suggestions. See, Zeidan [24–26] and Goncalves [27] for such applications and references of nanofluids. Scientific and technological phenomena are referred to using the terms magnetic field and porous media. These effects in fluid flow are utilized in several industrial and practical applications such as MHD power generators, the polymer industry, regenerative heat exchange, MHD flow meters and pumps, geothermal recovery, solar power collectors, and electrochemical processes (see [28–30]). Therefore, they play a significant role in fluid flow problems.

2. Physical model and governing equations

The two-dimensional motion with heat and mass transfer on the surface of grapheme nanoparticles with water is considered (see Figure 1). The terms ambient temperature and concentration T_∞ and C_∞ are keep as constants. The leading governing equations are provided as follows (see Mahabaleshwar [31–34] and Aly [35]):

$$\frac{\partial u}{\partial x}+\frac{\partial \mathrm{v}}{\partial y}=0, \tag{1}$$

$$u\frac{\partial u}{\partial x}+\mathrm{v}\frac{\partial u}{\partial y}=\frac{\mu_{eff}}{\rho_{nf}}\frac{\partial^2 u}{\partial y^2}-\left(\frac{\nu_{nf}}{K}+\frac{\sigma_{nf}{B_0}^2}{(\rho C_p)_{nf}}\right)u, \tag{2}$$

$$\begin{aligned} u\frac{\partial T}{\partial x}+\mathrm{v}\frac{\partial T}{\partial y}&=\frac{\kappa_{nf}}{(\rho C_p)_{nf}}\frac{\partial^2 T}{\partial y^2}-\frac{1}{(\rho C_p)_{nf}}\frac{\partial q_r}{\partial y}\\ &+\frac{\mu_{nf}}{(\rho C_p)_{nf}}\left(\frac{\partial u}{\partial y}\right)^2+\left\{\frac{\nu_{nf}}{K}+\frac{\sigma_{nf}{B_0}^2}{(\rho C_p)_{nf}}\right\}u^2 \end{aligned} \tag{3}$$

$$u\frac{\partial C}{\partial x}+\mathrm{v}\frac{\partial C}{\partial y}=D_B\frac{\partial^2 C}{\partial y^2}-R(C-C_\infty) \tag{4}$$

Boundary conditions (B. Cs) in terms of surface tension are as follows:

$$\sigma=\sigma_0\left[1-\gamma_T(T-T_\infty)-\gamma_C(C-C_\infty)\right], \tag{5}$$

where, the temperature and concentration surface tension coefficients are given as below:

$$\gamma_T=-\frac{1}{\sigma_0}\frac{\partial\sigma}{\partial T}\ \text{and}\ \gamma_C=-\frac{1}{\sigma_0}\frac{\partial\sigma}{\partial C}, \tag{6}$$

and the imposed conditions are:

$$\mu\frac{\partial u}{\partial y}=-\frac{\partial\sigma}{\partial x}=\sigma_0\left(\gamma_T\frac{\partial T}{\partial x}+\gamma_C\frac{\partial C}{\partial x}\right)\quad\text{at}\quad y=0. \tag{7}$$

The imposed conditions for dimensionless variable $X=x/L$are,

$$\begin{aligned} \mathrm{v}(x,y)&=\mathrm{v}_w\ T(x,y)=T_\infty+T_0X^2, C(x,y)\\ &=C_\infty+C_0X^2\ \text{ at }\ y=0,\ u(x,y)=0, T(x,y)\\ &=T_\infty, C(x,y)=C_\infty,\ \text{ as }\ y\to\infty. \end{aligned} \tag{8}$$

Here, $L=\frac{\mu\nu}{\sigma_0T_0\gamma_T}$ is the characteristic length.

Using approximation of Rosseland's solution, the q_r can be defined as (see [36–39]) as follows:

$$q_r=-\frac{4\sigma^*}{3k^*}\frac{\partial T^4}{\partial y}. \tag{9}$$

The term T^4extended on the basis of Taylor's series to yield (neglecting the terms of higher order),

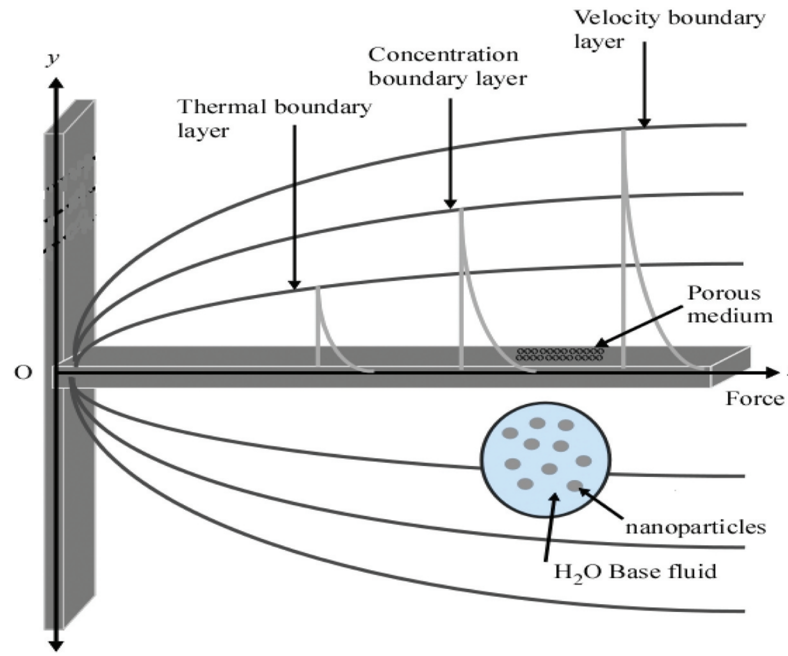

Figure 1. Physical sketch of the flow.

$$T^4 \cong 4T_\infty^3 T - 3T_\infty^4. \tag{10}$$

Then Eq. (3) becomes

$$u\frac{\partial T}{\partial x} + \mathrm{v}\frac{\partial T}{\partial y} = \frac{k_{nf}}{(\rho C_p)_{nf}}\frac{\partial^2 T}{\partial y^2} + \frac{16\sigma^* T_\infty^3}{3k^*(\rho C_P)_{nf}}\frac{\partial^2 T}{\partial y^2} + \frac{\mu_{nf}}{(\rho C_p)_{nf}}\left(\frac{\partial u}{\partial y}\right)^2 + \left\{\frac{\nu_{nf}}{K} + \frac{\sigma_{nf} B_0{}^2}{(\rho C_p)_{nf}}\right\}u^2 \tag{11}$$

Following similarity variables are used for further process:

$$\psi(\eta) = \nu_f X f(\eta), \eta = \tfrac{y}{L} u = \tfrac{\nu}{L} X f_\eta(\eta) \quad \mathrm{v} = -\tfrac{\nu}{L} f(\eta)$$
$$T(x,y) = T_\infty + T_0 X^2 \theta(\eta) \;\; C(x,y) = C_\infty + C_0 X^2 \phi(\eta) \tag{12}$$

Apply transformations as in Eq. (12) into Eqs. (2) - (4) to yield,

$$\Lambda f_{\eta\eta\eta} + D_1\left(ff_{\eta\eta} - f_\eta{}^2\right) - D_2\left(Da^{-1} + M\right)f_\eta = 0, \tag{13}$$

$$\frac{1}{\Pr}(D_4 + N_R)\theta_{\eta\eta} + D_3\left(f\theta_\eta - 2f_\eta\theta\right) + Ec\left[D_2 f_{\eta\eta}{}^2 + D_5\left(Da^{-1} + M\right)f_\eta{}^2\right] = 0 \tag{14}$$

$$\phi_{\eta\eta} + Sc\left[f\phi_\eta - \left(\beta + 2f_\eta\right)\phi\right] = 0 \tag{15}$$

B. Cs are also transformed as (See Aly and Ebaid [40])

$$f(0) = S \;\; f_{\eta\eta}(0) = -2(1 + Ma) \; f_\eta(\infty) = 0, \tag{16a}$$

$$\theta(0) = 1, \;\; \theta(\infty) = 0, \tag{16b}$$

$$\phi(0) = 1, \;\; \phi(\infty) = 0, \tag{16c}$$

Here, $Da^{-1} = \frac{L^2}{K}$ is the inverse Darcy number, $\Lambda = \frac{\mu_{eff}}{\mu_f}$ is Brinkman ratio, $M = \frac{\sigma_f B_0{}^2}{a_+ \nu_f}$ is the magnetic field, $N_R = \frac{16\sigma^* T_\infty{}^3}{3k_f k^*}$ is thermal radiation. $Ma = \frac{Ma_C}{Ma_T}$ is Marangoni number, where, $Ma_T = \frac{\sigma_0 \gamma_T T_0 L}{\alpha\mu}$ and $Ma_C = \frac{\sigma_0 \gamma_C C_0 L}{\alpha\mu}$ are thermal and solutal Marangoni number. $S = -\frac{\nu}{L}\nu_0$ is mass transpiration, $\beta = \frac{RL^2}{\nu}$ is chemical reaction parameter. The quantities D_i $i = 1$ to 5are described as below, where φ is volume fraction of graphene nanoparticle and the values of thermo physical properties seen in Table 1 (see Aly [41]).

$$D_1 = \frac{\rho_{nf}}{\rho_f} = 1 - \varphi + \varphi\left(\frac{\rho_s}{\rho_f}\right), D_2 = \frac{u_{nf}}{u_f} = \frac{1}{(1-\varphi)^{2.5}},$$
$$D_3 = \frac{(\rho C_P)_{nf}}{(\rho C_P)_f} = 1 - \varphi + \varphi\frac{(\rho C_P)_s}{(\rho C_P)_f},$$

$$D_4 = \frac{K_{nf}}{K_f} = \frac{K_s + 2K_f 2\varphi(K_s - K_f)}{K_s + 2K_f - \varphi(K_s - K_f)},$$
$$D_5 = \frac{\sigma_{nf}}{\sigma_f} = 1 + \frac{3(\frac{\sigma_s}{\sigma_f} - 1)\varphi}{\left(\frac{\sigma_s}{\sigma_f} + 2\right) - \left(\frac{\sigma_s}{\sigma_f} - 1\right)\varphi} \tag{17}$$

3. Solution of the model equations

We establish the analytical solution for the equations (1)–(4). Further, the analytical solution of equation (13),

Table.1. Quantities of graphene nanoparticle (see Aly [33]).

Physical properties	Base fluid Water(H_2O)	Graphene Nanoparticle (G)
ρ (kg/m^3)	997.1	2250
C_P $(J/kg\,K)$	4179	2100
k $(W/m\,K)$	0.613	2500
σ $(\Omega/m)^{-1}$	0.05	1×10^7

subjected to the boundary conditions as in equation (16a), is in the form,

$$f(\eta) = f_\infty + (S - f_\infty)Exp[-\delta\eta], \tag{18}$$

$$f_\infty = \frac{1}{D_1}\left(\Lambda\delta - D_2\frac{\{Da^{-1} + M\}}{\delta}\right), \tag{19}$$

$$f_\infty = S + \frac{2(1 + Ma)}{\delta^2}. \tag{20}$$

Upon using equations (19) and (20) leads to,

$$\frac{\Lambda}{D_1}\delta^3 - S\delta^2 - \frac{D_2}{D_1}\left(Da^{-1} + M\right)\delta - 2(1 + Ma) = 0. \tag{21}$$

Surface velocity is found to be,

$$f_\eta(0) = \frac{\Lambda}{D_1}\delta^2 - S\delta - \frac{D_2}{D_1}\left(Da^{-1} + M\right). \tag{22}$$

Now, introducing the new variable for temperature and concentration as (see Turkyilmazoglu [42]),

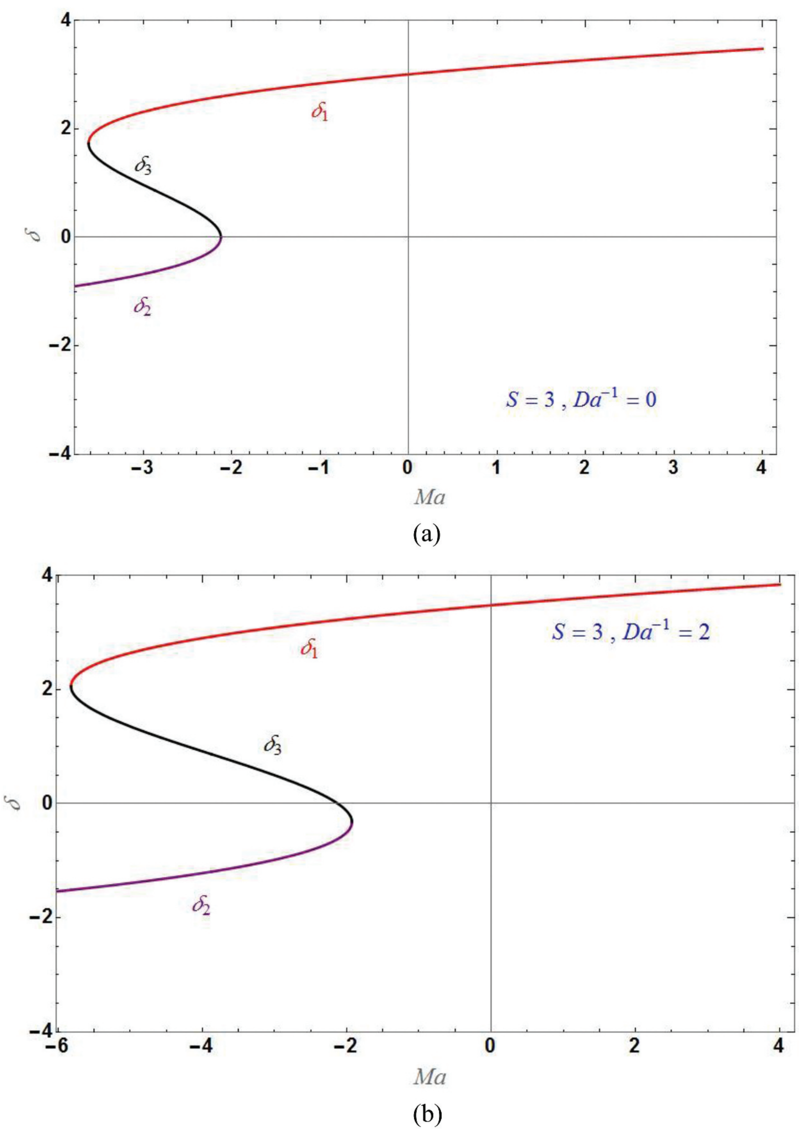

Figure 2. Solution domain δversus Marangoni number $Ma$for suction case with $\Lambda = 1, \varphi = 0.1$.

$$\varepsilon = \left(\frac{\Pr(S - f_\infty)}{\beta(D_4 + N_R)}\right) Exp(-\delta\eta) \text{ and}$$
$$\xi = \left(\frac{Sc(S - f_\infty)}{\delta}\right) Exp(-\delta\eta) \tag{23}$$

On using these in equations (14) and (15) will imply,

$$\varepsilon \frac{\partial^2\theta}{\partial\varepsilon^2} + (1 - D_3 a_1 - D_3\varepsilon)\frac{\partial\theta}{\partial\varepsilon} + 2\varepsilon_4\theta = -Ec^*\varepsilon, \tag{24a}$$

$$\xi \frac{\partial^2\phi}{\partial\xi^2} + (1 - a_2 - \xi)\frac{\partial\phi}{\partial\xi} + \left(2 + \frac{a_3}{\xi}\right)\phi = 0, \tag{24b}$$

where,

$$a_1 = \frac{\Pr f_\infty}{\delta(D_4 + N_R)},\ a_2 = \frac{Scf_\infty}{\delta}\ \ a_3 = -\frac{Sc\beta}{\delta^2},$$
$$Ec^* = -\frac{Ec\delta^2}{\Pr^2}(D_4 + N_R)\left(D_2\delta^2 + D_5\{Da^{-1} + M\}\right). \tag{25}$$

Further, the boundary conditions (16b) and (16c) will reduced to,

$$\theta(\varepsilon = -1) = 1, \quad \theta(\varepsilon = 0) = 0, \tag{26a}$$

$$\phi(\xi = -1) = 1, \quad \phi(\xi = 0) = 0. \tag{26b}$$

On solving equation (24a) and (24b) with boundary conditions (26a) and (26b) to obtain the following solutions:

$$\theta(\eta) = (1 - b_2)Exp(-b_1\delta\eta)\frac{L(2 - b_1,\ b_1,\ D_3\varepsilon)}{L(2 - b_1,\ b_1,\ -D_3\varepsilon_0)} + b_2\varepsilon^2, \tag{27}$$

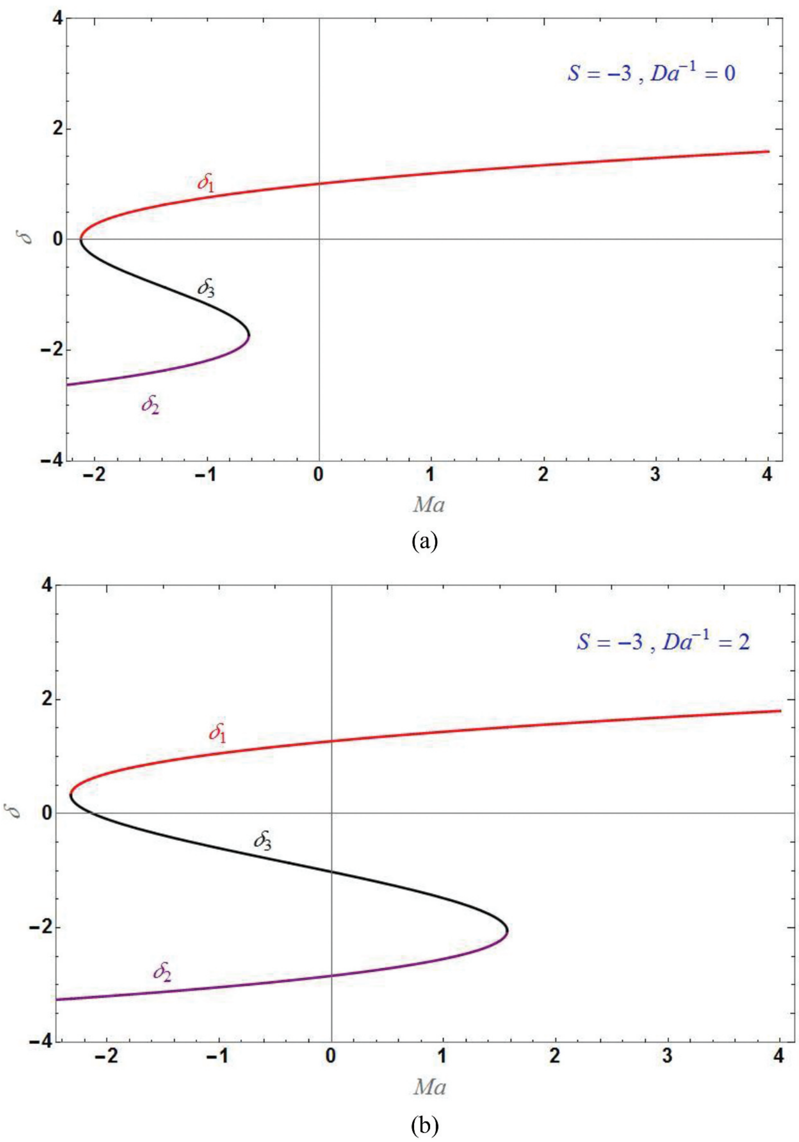

Figure 3. Solution domain δversus Marangoni number $Ma$for injection case with $\Lambda = 1, \varphi = 0.1$.

$$\phi(\eta) = Exp(-b_4\delta\eta)\frac{L(2-b_4,\ b_3,\ \xi)}{L(2-b_4,\ b_3,\ \xi_0)}, \qquad (28)$$

where,

$$b_1 = D_3a_1, b_2 = \frac{D_3E_C{}^*}{2D_3a_1 - 4}, b_3 = \sqrt{a_2{}^2 - 4a_3},$$
$$b_4 = \frac{a_2}{2} + \frac{\sqrt{a_2{}^2 - 4a_3}}{2}, \varepsilon_0 = \left(\frac{\Pr(S - f_\infty)}{\delta(D_4 + N_R)}\right),$$
$$\xi_0 = \left(\frac{Sc(S - f_\infty)}{\delta}\right)$$

are the dummy variables and $L(a, b, z)$ is Laguerre polynomial.

4. Results and discussion

The current work considers two-dimensional incompressible flow over porous media with Marangoni boundary conditions by adding graphene nanoparticles to the flow. The ODEs are solved analytically to yield exponential and hypergeometric functions. Using graphs, the impact of various parameters like the Marangoni and inverse Darcy numbers, the Brinkman ratio, the Prandtl number, and the Eckert number is analysed. The addition of graphene nanoparticles can act as heaters upon an increase in their solid volume fraction, Eckert numbers, and injection, and can act as coolers upon an increase in suction.

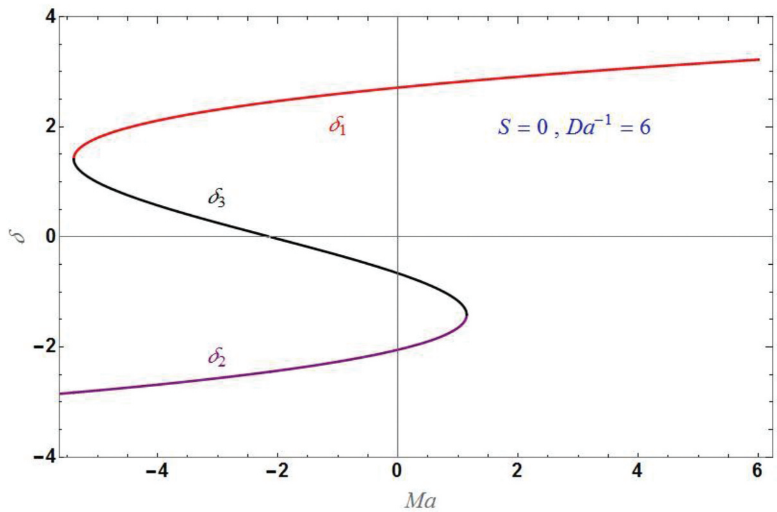

(a)

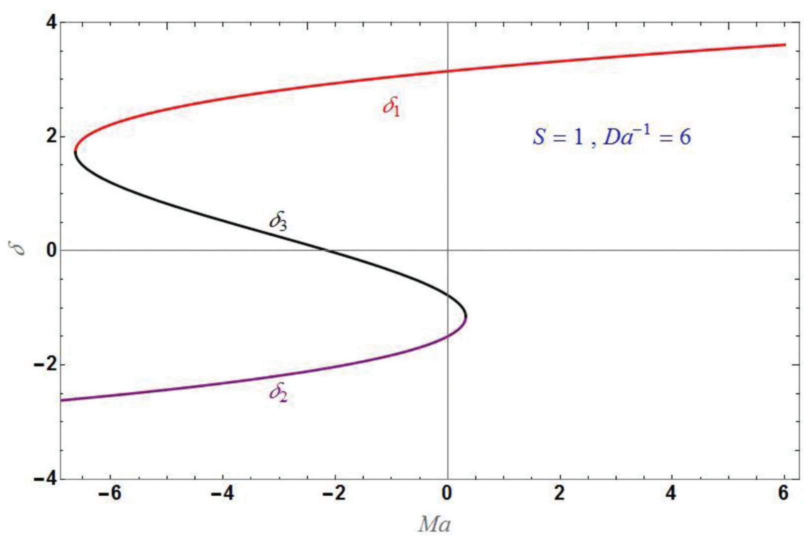

(b)

Figure 4. Solution domain δversus Marangoni number $Ma$for (a) impermeable case and (b) suction case with $\Lambda = 1, \varphi = 0.1$.

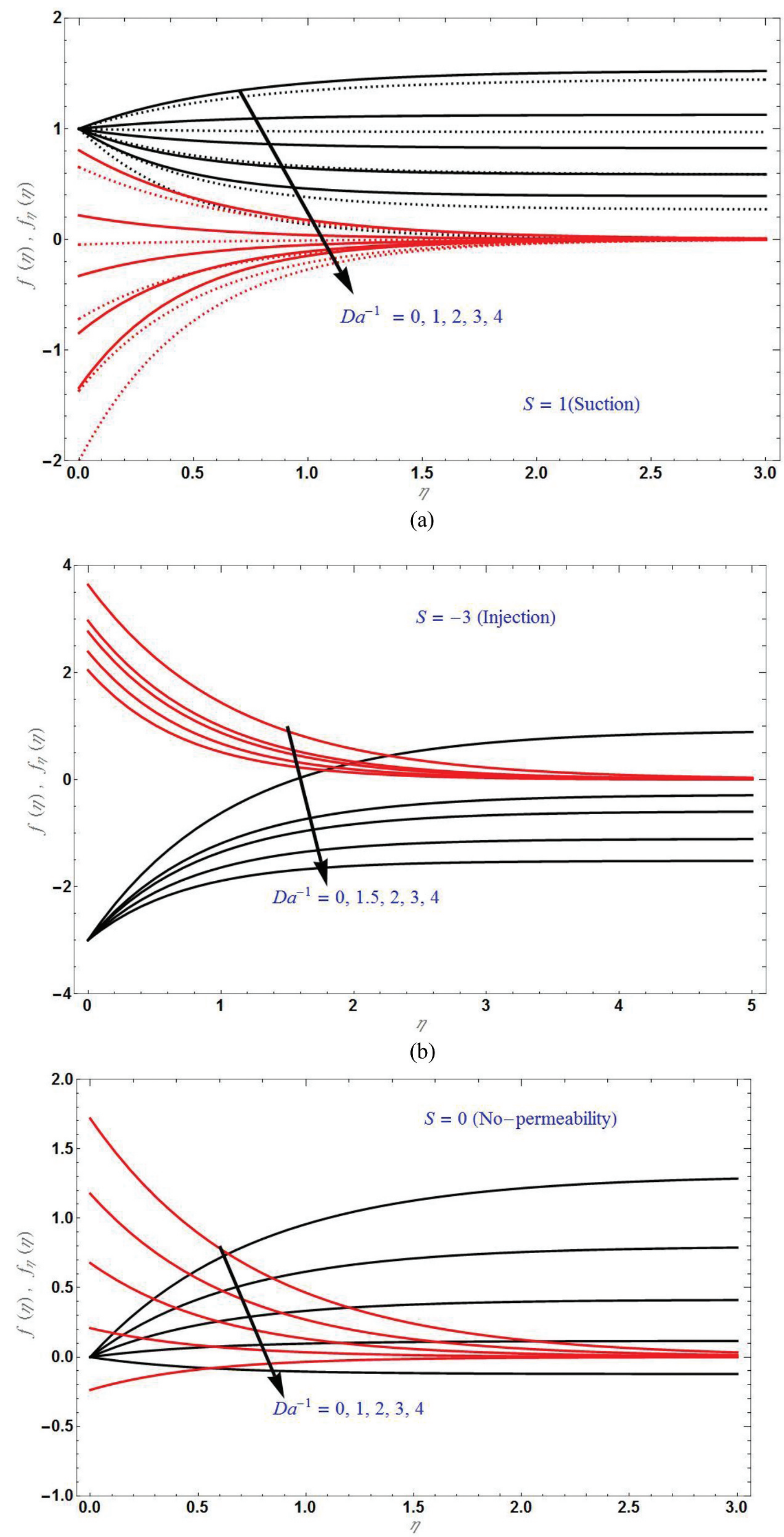

Figure 5. $f(\eta)$ and $f_n(\eta)$ velocities for different values at (a) $S>0$, (b) $S<0$ and (c) $S=0$ with $Ma=1, \Lambda=2, \varphi=0.1$.

The present work is well-argued and aligns with many existing works:

(a) If$\varphi = 0$ and $\Lambda = 1, Ec = 0$, the present work transforms to the work ofMahabaleshwar et al. [31] when$I = 0$.
(b) If $\Lambda = 1, Ec = 0$, then the present work transforms to the work of Alyand Ebaid [40].
(c) If $\Lambda = 1, Da^{-1} = Ec = N_R = 0$, then the present work transforms to the work of Remeli et al. [43].
(d) If $\Lambda = 1, Ec = 0$, then the present work transforms to work of Rashid et al [44]. which is solved numerically.
(e) Khan et al. [45] concentrated on combined effects of buoyancy forces, elasticity, suction or injection, first-order slip, magnetic effects, nanoparticle motion and second-order slip on a mixed convectionflow in the vicinity of a stagnation point past a porousstretching/shrinking surface.

Figure 2–4 demonstrate the physical solution to the flow problem. The three roots of equation (21) are demonstrated for varying Marangoni number. When the Ma varies, the physical solution also adjusts appropriately. Additionally, the interaction between S and the Da^{-1} has a direct impact on whether a physical solution exists. The correct physical solution field can be obtained by properly selecting Da^{-1} and S properly. Figure 2 depicts the solution domain for the suction case, where Figures 2(a,b) examine it with and without Da^{-1}respectively. Further,

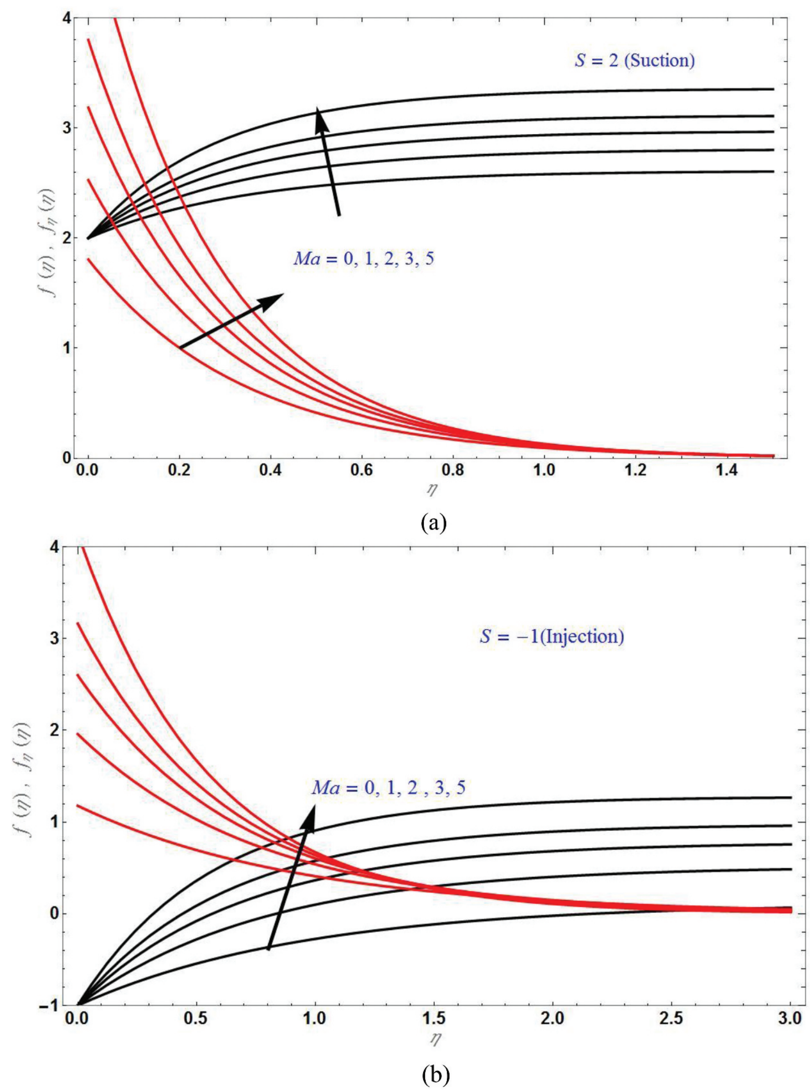

Figure 6. $f(\eta)$ and $f_n(\eta)$ an velocities for different values at a) $S > 0$, and (b) $S < 0$ with $Da^{-1} = 1, \Lambda = 2, \varphi = 0.1$.

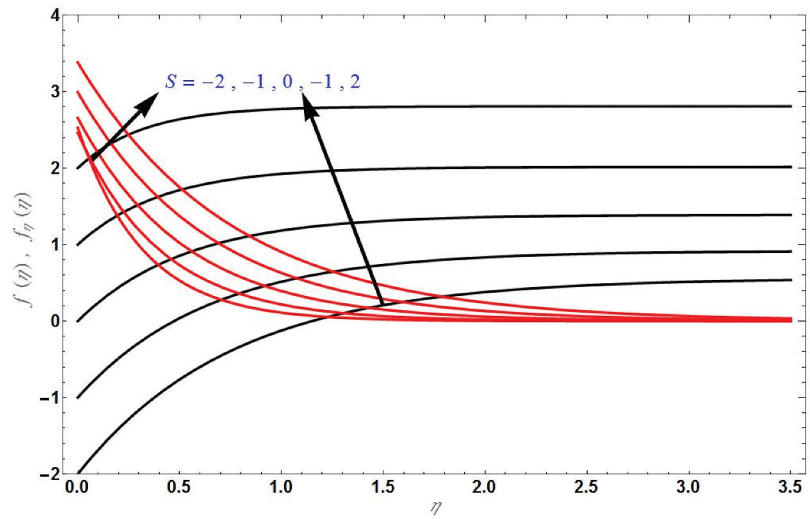

Figure 7. $f(\eta)$and $f_\eta(\eta)$velocities for different values of $S$for a) $S > 0$, and (b) $S < 0$ with $Ma = Da^{-1} = 1, \Lambda = 1, \varphi = 0.1$.

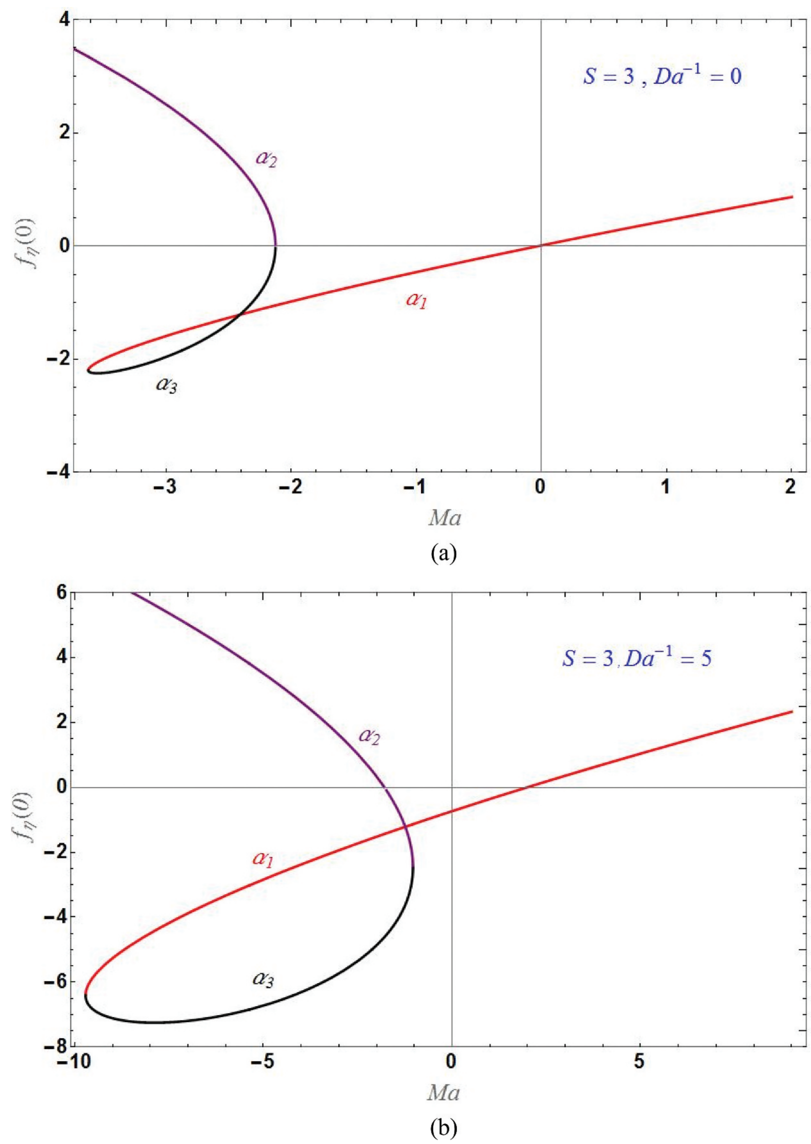

Figure 8. Surface velocity $f_\eta(0)$ versus Marangoni number Ma with $\Lambda = 1, \varphi = 0.1$.

Figure 3 depicts the solution domain for injection case, where Figure 3(a,b) examine it with and without Da^{-1}respectively for different choices of other controlling parameters. Figure 4(a,b) show the difference between the solution domain with and without mass transpiration.

Figure 5–7 demonstrate transverse $f(\eta)$and axial $f_\eta(\eta)$velocities. In Figure 5, there is an examination of $f(\eta)$and $f_\eta(\eta)$for different values of Da^{-1}in suction, injection, and impermeable cases, respectively, in Figure 5(a,c). In Figure 5(a) dotted lines show the flow without nanofluid, and solid lines demonstrate the flow with nanofluid. We can conclude that as Da^{-1} increases, both transverse and axial velocities decrease. In Figure 6, there is an examination of $f(\eta)$and $f_\eta(\eta)$for different Ma values at $S>0$, and $S<0$cases respectively, in Figure 6(a,b). We can conclude that as Ma increases, both transverse and axial velocities increase. Figure 7 examines the $f(\eta)$and $f_\eta(\eta)$for different values of S, can be further observed that both $f(\eta)$and $f_\eta(\eta)$are increasing with an increase in S. In addition to this, the mass transpiration parameter, together with the inverse Darcy number produces more impact on the velocity boundary in comparison to the choice of the inverse Darcy number alone.

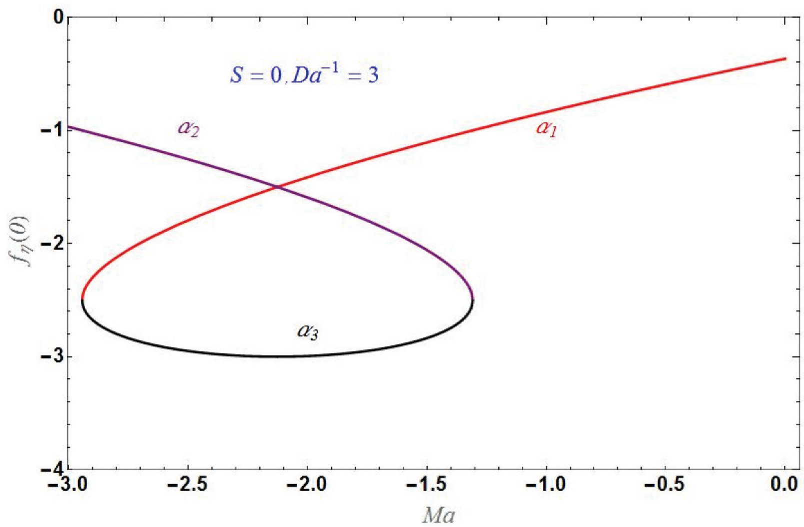

Figure 9. Surface velocity $f_\eta(0)$ versus Marangoni number Ma with $\Lambda = 2, \varphi = 0.1$.

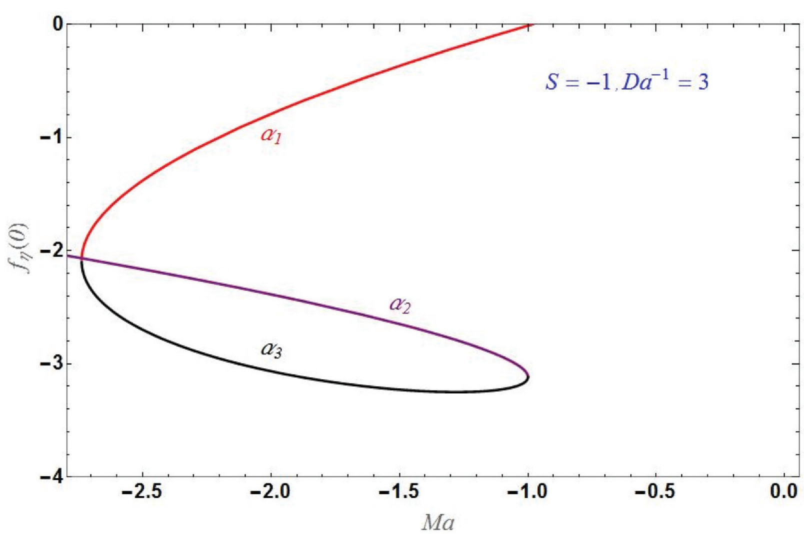

Figure 10. Surface velocity $f_\eta(0)$ versus Marangoni number Ma with $\Lambda = 2, \varphi = 0.1$.

The usage of magnetic field and porous media plays a significant role in fluid flow, as these effects in the fluid flow are used in several industrial and practical applications like MHD power generators, polymer industry, regenerative heat exchange, MHD flow meters and pumps, geothermal recovery, solar power collectors, electrochemical processes, etc. Heat transfer, or heat loss or gain is prevented by porous medium and more induced flows emerge from Marangoni convection. It's worthwhile to note that thermosolutal Marangoni convection has important uses in the production of semiconductors and in the metallurgical sectors, where its importance can be seen in the control of heat and mass transfer in metallic fluids.

The porosity of the medium is a key element in determining the results of the processes in practical issues including geosciences, glassblowing, oil and gas recovery, and catalytic reactors. The Darcy law, which takes into account the pressure gradient, fluid viscosity, and gravitational force, governs convective fluxes in porous media. The effects of inertia forces and heat transmission through porous media are not taken into account in the theoretical model; they only become important when the momentum is very high. However, in the Darcy-Brinkman medium, without a driving pressure gradient, a well-positioned porous matrix is sufficient to obstruct the flow of a viscous fluid.

For various selections of Ma, Figures 8 and 10 show the relationship between the trajectories of the same

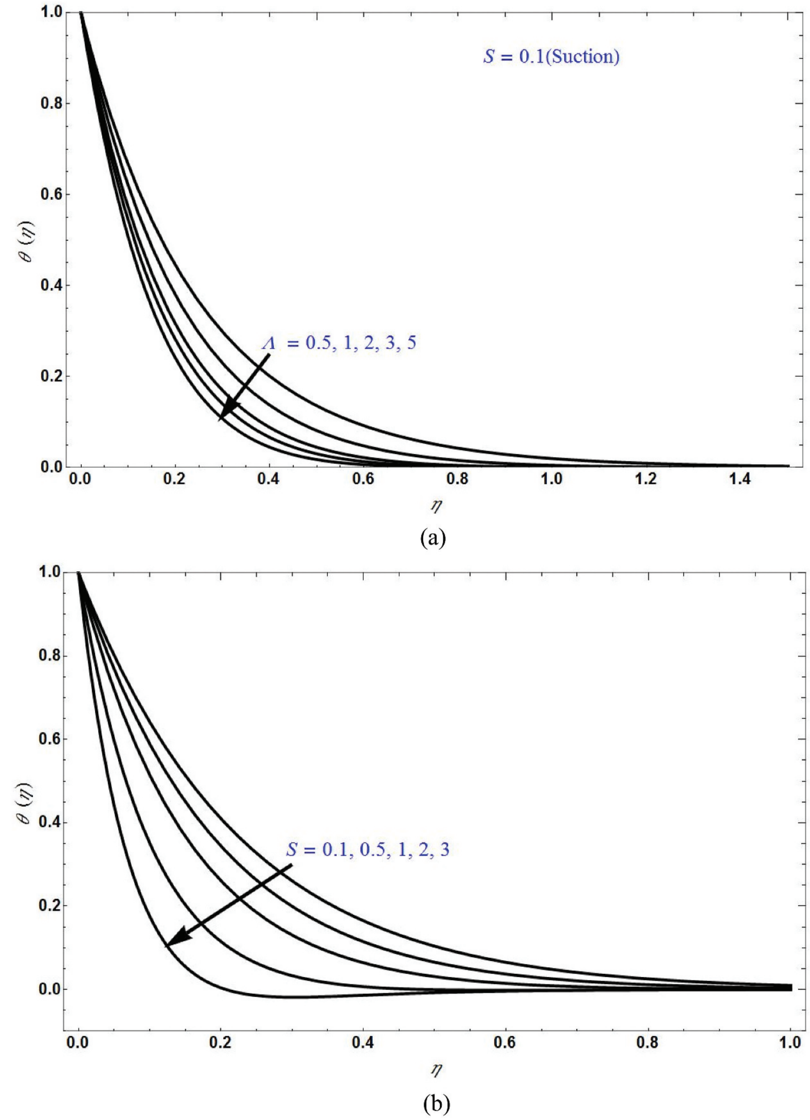

Figure 11. $\theta(\eta)$ verses η for various choices of (a) Λ and (b) S With $M = Ma = 1, Da^{-1} = 0.2, Ec = 0.1, N_R = 0.2, \Pr = 6.2, \varphi = 0.1$.

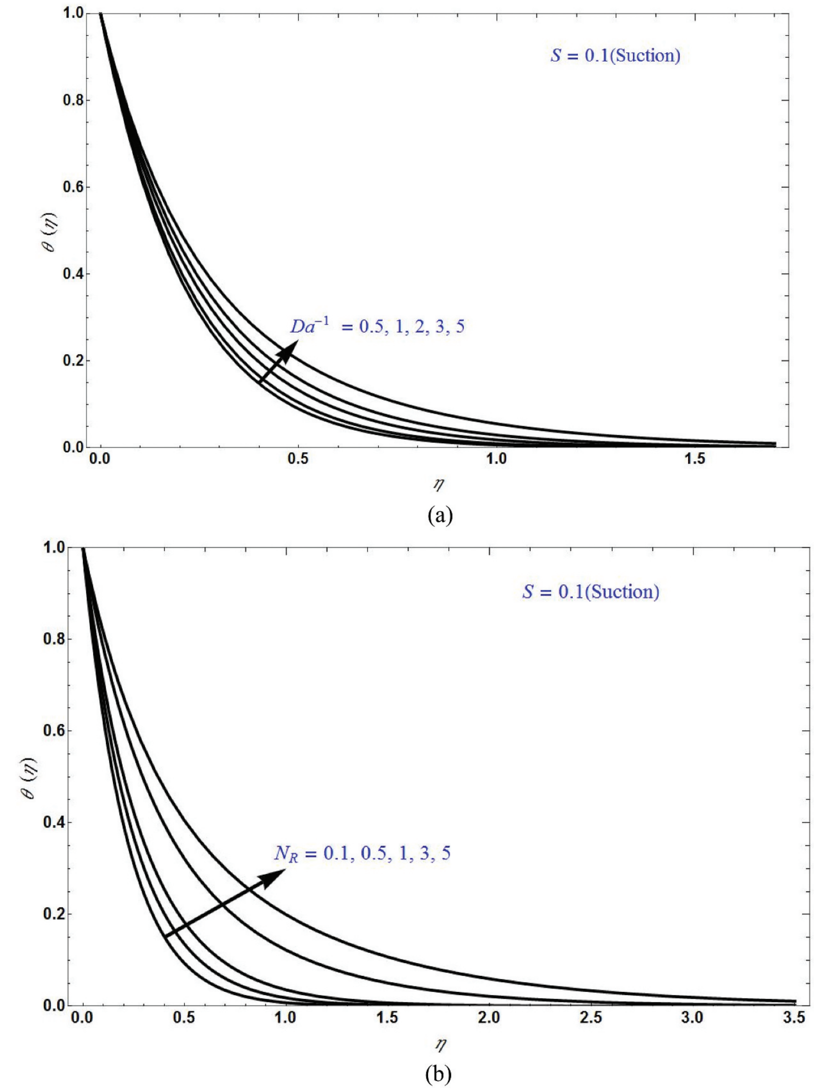

Figure 12. Temperature distribution $\theta(\eta)$ for various (a) inverse Darcy number (Da^{-1}) with $N_R = 0.2$ and (b) radiation parameter (N_R) with $M = Ma = \Lambda = 1, Ec = 0.1, \Pr = 6.2, \varphi = 0.1$.

surface velocity $f_\eta(0)$connected to the three roots. When $Da^{-1}$and S are combined, the ranges of physical and non-physical surface velocities correspond, respectively, to positive and negative roots. Figure 8 examines it for suction case, with and without Da^{-1}respectively; in Figures 8(a,b) and 9 examines it for impermeable case with $Da^{-1}$and Figure 10 for injection case with Da^{-1}.

Figure 11 and 12 demonstrate the temperature distribution$\theta(\eta)$. In Figure 11, there is an examination of $\theta(\eta)$in suction case by varying Brinkman ratio(Λ) and mass transpiration, respectively, in Figure 11(a,b). We can conclude that $\theta(\eta)$will decrease as $\Lambda$and S increases. In Figure 12 there is an examination of $\theta(\eta)$in suction case, by varying inverse Darcy number(Da^{-1}) and radiation (N_R)respectively, in Figure 12(a,b). We can conclude that the $\theta(\eta)$will decrease as $Da^{-1}$and $N_R$increases.

Figure 13 and 14 demonstrate the concentration field$\phi(\eta)$. In Figure 13, there is an examination of $\phi(\eta)$in suction case by varying Sc and β respectively, in Figure 13(a,b). We can conclude that$\phi(\eta)$will decrease as $Sc$and βincreases. In Figure 14 there is an examination of $\phi(\eta)$by varying S and Ma respectively, in Figure 14(a,b). We can conclude that the $\phi(\eta)$will decreases as S and Ma increase. Chemical reaction will thin the thermal boundary layer.

5. Conclusions and future works

The investigation performs a study of 2-D flow transfer over porous media with mass transpiration and Marangoni boundary conditions by adding graphene nanoparticles to the flow. The governing equations are

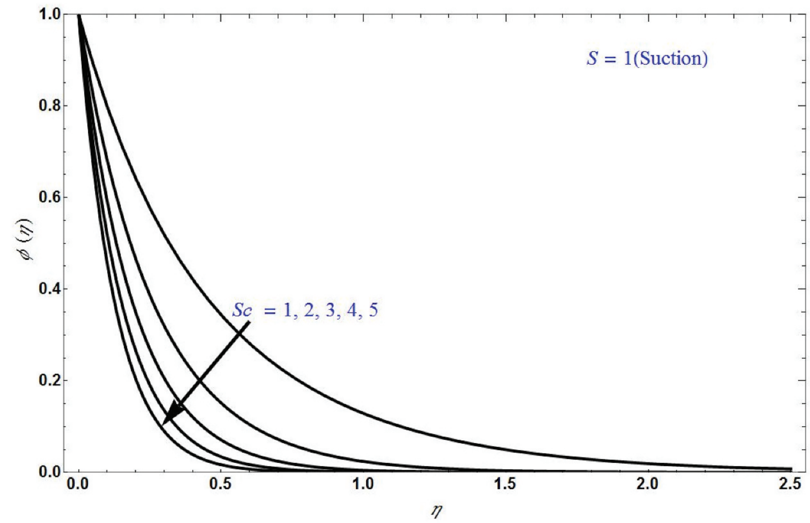

(a)

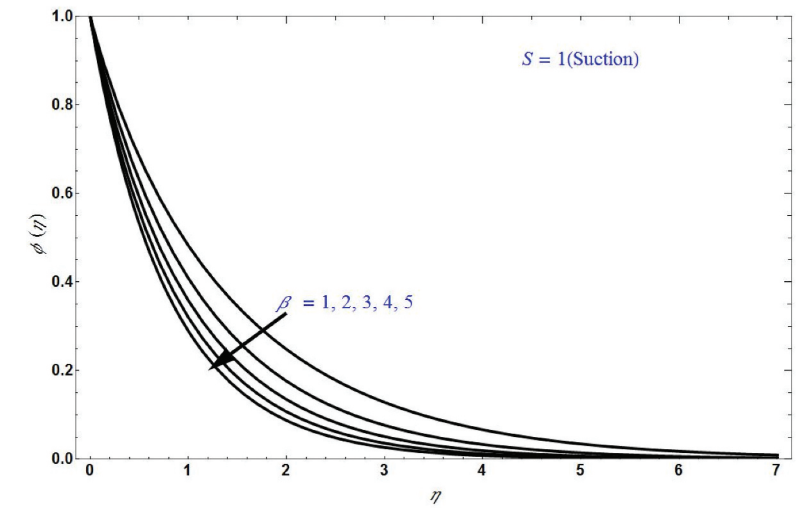

(b)

Figure 13. Concentration field $\phi(\eta)$ for various (a) Schmidt number (Sc) with $\beta = 0.2$ and (b) chemical reaction parameter (β) with keeping other parameters as.

solved to obtain the solutions in terms of exponential and hypergeometric functions. Using graphs, the following observation can be made:

- The nanoparticles of graphene are mixed in water to improve thermal efficiency. The existence of graphene water nanofluid will enhance thermal efficiency in a better way than the base fluid.
- The addition of graphene nanoparticles can act as heaters upon an increase in their solid volume fraction, Eckert number, and injection, and they can act as coolers upon an increase of suction.
- The interaction between S and Da^{-1}has a direct impact on whether a physical solution exists.
- As the Marangoni number increases, both transverse and axial velocities increase.
- As the inverse Darcy number increases, both transverse and axial velocities decrease.
- Both transverse and axial velocities increase with an increase in mass transpiration.
- The temperature distribution will decrease as the Brinkman ratio or mass transpiration increases, and it will decrease as the inverse Darcy number or radiation parameter increases.

In the future some may study the flow by adding ternary hybrid nanoparticles of different shapes. This study, therefore, can be further estimated by adding different boundary conditions, such as slip boundary conditions.

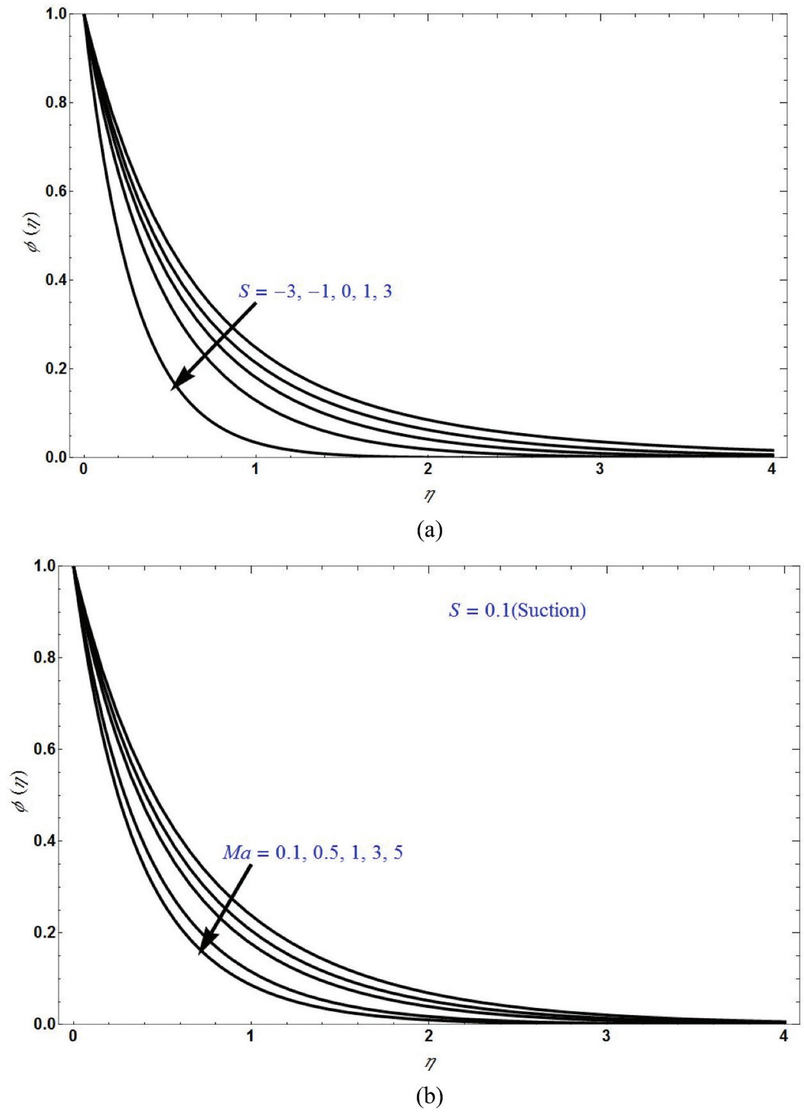

Figure 14. Concentration field $\phi(\eta)$ for different values of (a) mass (S) transpiration with $Ma = 1$ and (b) Marangoni (Ma) number keeping other parameters as $Da^{-1} = 0.5, \beta = 0.2, Sc = \Lambda = 1, \varphi = 0.1$.

Nomenclature

Symbol	Description	S.I. Unit
Latin symbols		
B_0	Strength of magnetic field	$[wm^{-2}]$
C	Concentration	$[mol/m^3]$
C_P	Specific heat at constant pressure	$[JKg^{-1}K^{-1}]$
$_{DB}$	Parameter of mass diffusivity	$[m^2s^{-1}]$
Ec	Eckert number	$[-]$
f	dimensionless variable for velocity	$[-]$
k^*	Coefficient of mean absorption	$[m^{-2}]$
K	Porous medium Permeability	$[m^{-2}]$
L	Laguerre polynomial	$[-]$
Pr	Prandtl number	$[-]$
q_r	radiative heat flux	$[Wm^{-2}]$

(*Continued*)

(Continued).

Nu_x	local Nusselt number	$[-]$
M	magnetic parameter	$[-]$
Ma	Marangoni number	$[-]$
R	coefficient of chemical reaction	$[-]$
T	temperature	$[K]$
$S>0/<0$	suction/injection velocity	$[-]$
Sc	Schmidt number	$[-]$
(u, v)	velocities	$[ms^{-1}]$
v_w	velocity at the wall	$[ms^{-1}]$
(x, y)	coordinate axes	$[m]$
Greek symbols		
β	chemical reaction parameter	$[-]$
α	thermal diffusivity	$[m^2s^{-1}]$
κ	thermal conductivity of fluid	$[WKg^{-1}K^{-1}]$
η	similarity variable	$[-]$
θ	dimensionless variable for temperature	$[-]$
ϕ	dimensionless variable for concentration	$[-]$
μ_{eff}	effective viscosity	$[-]$
σ^*	Stefan-Boltzmann constant	$[-]$
φ	Volume fraction	$[-]$
Λ	Brinkman ratio	$[-]$
ψ	Stream function	$[-]$
Subscripts		
∞	ambient condition	$[-]$
f	base fluid	$[-]$
nf	nanofluid	$[-]$

Acknowledgments

T. A. is thankful to Council of Scientific and Industrial Research (CSIR), New Delhi, INDIA for financial support in the form of Senior Research Fellowship: File No. 09/1207(0003)/2020-EMR-I. L.M.P. acknowledges partial financial support from ANID through Convocatoria Nacional Subvención a Instalación en la Academia Convocatoria Año 2021, Grant SA77210040. Support provided through Davangere University, India, Universidad de Tarapacá, Chile, and the German Jordanian University, Amman, Jordan, is highly acknowledged and appreciated by the authors.

Disclosure statement

The authors declare that they have no known competing financial interests or personal relationships that could have appeared to influence the work reported in this paper.

Funding

The work was supported by the ANID through Convocatoria Nacional Subvención a Instalación en la Academia Convocatoria Año 2021 [SA77210040].

Notes on contributors

T. Anusha received M. Sc degree in Mathematics from Kuvempu University, Shimoga, Karnataka in 2017. She qualified KSET in 2017 December and NET-JRF in 2018 December. Further she joined Ph.D. in Davangere University under the guidance of Prof. U. S. Mahabaleshwar in 2020 February. Her research interests are on fluid mechanics topics, heat and mass transfer, boundary layer flows. She has published 22 research papers.

L. M. Pérez (Assistant Professor at Universidad de Tarapacá) received a B.Sc. degree in physics from Universidad del Valle (Cali, Colombia) with the first rank of her promotion. She holds a Ph.D. in complex systems from Universidad de Navarra (Pamplona, Spain). Her areas of research interests are fluid mechanics, condensed matter and computational physics. She has gotten several competitive Grants as a PI as well as CI. She has published more than 100 research papers and mentored master students.

U. S. Mahabaleshwar (Professor in Davangere University) received M. Sc degree from Gulbarga University, Karnataka, India in 2000. His areas of research interests are Rayleigh-Benard convection problems, Linear and nonlinear stretching sheet problems, heat and mass transfer problems in Newtonian and Non-Newtonian fluids, Double diffusive convection. He is the reviewer and editor of many reputed journals. He has published more than 180 research papers and produced five Ph. D students and one M. Phil student.

D. Zeidan is a Full Professor of Applied and Computational Mathematics at the German Jordanian University, Amman, Jordan, and Elected Fellow of the European Society of

Computational Methods in Sciences and Engineering. An active researcher in developing mathematical and numerical tools of multiphase fluid flow problems for several years, he is recognized for research contributions in applied and computational mathematics with multiphase flows including his creative approaches to teaching and research. His work has been highly interdisciplinary, involving international collaborations with applied and computational researchers. He serves on several expert review panels, as Technical Editor and Reviewer for several peer-reviewed journals and as Member of several program committees of technical conferences around the world.

ORCID

D. Zeidan http://orcid.org/0000-0001-9080-0308

Data availability statement

Data sharing is not applicable to this article.

References

[1] Turkyilmazoglu M. Multiple solutions of heat and mass transfer of MHD slip flow for the viscoelastic fluid over a stretching sheet. Int J Ther Sci. 2011;50 (11):2264–2276. doi: 10.1016/j.ijthermalsci.2011.05.014

[2] Fang TG, Wang FJ, Gao B. Unsteady magnetohydrodynamic stagnation point flow—closed-form analytical solutions. Appl Math Mech-Engl Ed. 2019;40 (4):449–464. doi: 10.1007/s10483-019-2463-7

[3] Crane LJ. Flow past a stretching plate. KurzeMitteilungen-Brief Reports. 1970;21(4):645–647. doi: 10.1007/BF01587695

[4] Hamad MAA. Analytical solution of natural convection flow of a nanofluid over a linearly stretching sheet in the presence of magnetic field. International Communications in Heat and Mass Transfer. 2011;38(4):487–492. doi: 10.1016/j.icheatmasstransfer.2010.12.042

[5] Fang T, Zhang J. Closed-form exact solutions of MHD viscous flow over a shrinking sheet. Commun Nonlinear Sci Numer Simul. 2009;14(7):2853–2857. doi: 10.1016/j.cnsns.2008.10.005

[6] Mahabaleshwar US. Stretching sheet and convective instability problems in Newtonian, micropolar and viscoelastic liquids. [Ph.D Thesis], Bangalore University, India, 2005.

[7] Mahabaleshwar US, Sneha KN, Chan A, et al. An effect of MHD fluid flow heat transfer using CNTs with thermal radiation and heat source/sink across a stretching/shrinking sheet. Int J Heat Mass Transf. 2022;135:106080. doi: 10.1016/j.icheatmasstransfer.2022.106080

[8] Wang CY. The three-dimensional flow due to a stretching flat surface. Phys Fluids. 1984;27 (8):1915–1917. doi: 10.1063/1.864868

[9] Anusha T, Mahabaleshwar US, Sheikhnejad Y. An MHD of nanofluid flow over a porous stretching/shrinking plate with mass transpiration and Brinkman ratio. Transp Porous Media. 2021;142(1):333–352. doi: 10.1007/s11242-021-01695-y

[10] Mahabaleshwar US, Vishalakshi AB, Ndi Azese M. The role of Brinkman ratio on non-Newtonian fluid flow due to a porous shrinking/stretching sheet with heat transfer. Eur J Mechanics/B Fluids. 2022;92:153–165. doi: 10.1016/j.euromechflu.2021.12.003

[11] Sneha KN, Mahabaleshwar US, Bennacer R, et al. Darcy Brinkman equations for hybrid dusty nanofluid flow with heat transfer and mass transpiration. Computation. 2021;9 (11):118. doi: 10.3390/computation9110118

[12] Zhao M, Wang S, Wang H, et al. Darcy–Brinkman bio-thermal convection in a suspension of gyrotactic microorganisms in a porous medium. Neural Comput Appl. 2019;31(4):1061–1067. doi: 10.1007/s00521-017-3137-y

[13] Zhao M, Wang S, Li SC, et al. Chaotic Darcy-Brinkman convection in a fluid saturated porous layer subjected to gravity modulation. Results Phys. 2018;9:1468–1480. doi: 10.1016/j.rinp.2018.04.047

[14] Merkin JH. On dual solutions occurring in mixed convection in a porous medium. J Eng Math. 1986;20 (2):171–179. doi: 10.1007/BF00042775

[15] Mahabaleshwar US, Nagaraju KR, Vinay Kumar PN, et al. Effects of Dufour and soret mechanisms on MHD mixed convective-radiative non-Newtonian liquid flow and heat transfer over a porous sheet. J Therm Sci Eng Prog. 2020;16:100459. doi: 10.1016/j.tsep.2019.100459

[16] Rohni AM, Ahmad S, Pop I, et al. Unsteady mixed convection boundary-layer flow with suction and temperature slip effects near the stagnation point on a vertical permeable surface embedded in a porous medium. Transp Porous Media. 2012;92(1):1–14. doi: 10.1007/s11242-011-9883-x

[17] Khan U, Shafiq A, Zaib A, et al. Hybrid nanofluid on mixed convective radiative flow from an irregular variably thick moving surface with convex and concave effects. Case Stud Thermal Eng. 2020;21:100660. doi: 10.1016/j.csite.2020.100660

[18] Yacob NA, Ishak A, Pop I, et al. Boundary layer flow past a stretching/shrinking surface beneath an external uniform shear flow with a convective surface boundary condition in a nanofluid. Nanoscale Res Lett. 2011;6 (1):314. doi: 10.1186/1556-276X-6-314

[19] Arifin NM, Nazar R, Pop I. Non-isobaric Marangoni boundary layer flow Cu, Al2O3 and TiO2 nanoparticles in a water-based fluid. Meccanica. 2011;46(4):833–843. doi: 10.1007/s11012-010-9344-6

[20] Napolitano LG Marangoni boundary layers, Proceedings of the 3rd European Symposium on Material Science in Space. Grenoble. ESA SP-142, Paris, June 1979.

[21] Chamkha AJ, Pop I, Takhar HS. Marangoni mixed convection boundary layer flow. Meccanica. 2006;41 (2):219–232. doi: 10.1007/s11012-005-3352-y

[22] Mudhaf AA, Chamkha AJ. Similarity solutions for MHD thermosolutal Marangoni convection over a flat surface in the presence of heat generation or absorption effects. Heat Mass Transfer. 2005;42(2):112–121. doi: 10.1007/s00231-004-0611-8

[23] Choi SUS, Eastman JA. Enhancing thermal conductivity of fluids with nanoparticles. Am Soc Mech Eng Fluids Eng Div FED. 1995;231:99–105.

[24] Zeidan D, Romenski E, Slaouti A, et al. Numerical study of wave propagation in compressible two-phase flow. Int J Numer Methods Fluids. 2007;54(4):393–417. doi: 10.1002/fld.1404
[25] Zeidan D, Bähr P, Farber P, et al. Numerical investigation of a mixture two-phase flow Model in two-dimensional space. Comput Fluids. 2019;181:90–106. doi: 10.1016/j.compfluid.2018.12.013
[26] Zeidan D, Zhang LT, Goncalves E. High-resolution simulations for aerogel using two-phase flow equations and Godunov methods. Int J Appl Mech. 2020;12(5):2050049. doi: 10.1142/S1758825120500490
[27] Goncalves E, Zeidan D. Numerical simulation of unsteady cavitation in liquid hydrogen flows. Int J Eng Systems Modelling Simul. 2017;9(1):41–51. doi: 10.1504/IJESMS.2017.081736
[28] Shi QH, Shabbir T, Mushtaq M, et al. Modelling and numerical computation for flow of micropolar fluid towards an exponential curved surface: a Keller box method. Sci Rep. 2021;11(1):16351. doi: 10.1038/s41598-021-95859-x
[29] Dawar A, Shah Z, Tassaddiq A, et al. Joule heating in magnetohydrodynamic micropolar boundary layer flow past a stretching sheet with chemical reaction and microstructural slip. Case Stud Thermal Eng. 2021;25:100870. doi: 10.1016/j.csite.2021.100870
[30] Shah Z, Shutaywi M, Dawar A, et al. Impact of Cattaneo-Christov heat flux on non-isothermal convective micropolar fluid flow in a hall MHD generator system. J Mater Res Technol. 2020;9(3):5452–5462. doi: 10.1016/j.jmrt.2020.03.071
[31] Mahabaleshwar US, Nagaraju KR, Vinay Kumar PN, et al. Effect of radiation on thermosolutal Marangoni convection in a porous medium with chemical reaction and heat source/sink. Phys Fluids. 2020;32(11):113602. doi: 10.1063/5.0023084
[32] Vinay Kumar PN, Mahabaleshwar US, Nagaraju KR, et al. Mass transpiration in magneto-hydrodynamic boundary layer flow over a superlinear stretching sheet embedded in porous medium with slip. J Porous Media. 2019;22(8):1015–1025. doi: 10.1615/JPorMedia.2019025664
[33] Mahabaleshwar US, Anusha T, Sakanaka PH, et al. Impact of inclined Lorentz force and Schmidt number on chemically reactive Newtonian fluid flow on a stretchable surface when Stefan blowing and thermal radiation are significant. Arabian J Sci Eng. 2021;46(12):12427–12443. doi: 10.1007/s13369-021-05976-y
[34] Mahabaleshwar US, Vinay Kumar PN, Nagaraju KR, et al. A new exact solution for the flow of a fluid through porous media for a variety of boundary conditions. Fluids. 2019;4(3):125. doi: 10.3390/fluids4030125
[35] Aly EH, Pop I. MHD flow and heat transfer near stagnation point over a stretching/shrinking surface with partial slip and viscous dissipation: hybrid nanofluid versus nanofluid. Powder Technol. 2020;367(18):192–205. doi: 10.1016/j.powtec.2020.03.030
[36] Rosseland S. Astrophysik and atom theoretische Grundlagen. Berlin: Springer- Verlag; 1931.
[37] Cortell R. Radiation effects for the Blasius and Sakiadis flows with a convective surface boundary condition. Appl Math Comput. 2008;206(2):832–840. doi: 10.1016/j.amc.2008.10.001
[38] Anusha T, Huang HN, Mahabaleshwar US. Two dimensional unsteady stagnation point flow of Casson hybrid nanofluid over a permeable flat surface and heat transfer analysis with radiation. J Taiwan Inst Chem Eng. 2021;127:79–91. doi: 10.1016/j.jtice.2021.08.014
[39] Xenos MA, Petropoulou EN, Siokis A, et al. Solving the nonlinear boundary layer flow equations with pressure gradient and radiation. Symmetry. 2020;12(5):710. doi: 10.3390/sym12050710
[40] Aly EH, Ebaid A. Exact analysis for the effect of heat transfer on MHD and radiation Marangoni boundary layer nanofluid flow past a surface embedded in a porous medium. J Mol Liq. 2016;215:625–639. doi: 10.1016/j.molliq.2015.12.108
[41] Aly EH. Dual exact solutions of graphene-water nanofluid flow over stretching/shrinking sheet with suction/injection and heat source/sink: critical values and regions with stability. Powder Technol. 2019;342:528–544. doi: 10.1016/j.powtec.2018.09.093
[42] Turkyilmazoglu M. Exact analytical solutions for heat and mass transfer of MHD slip flow in nanofluids. Chem Eng Sci. 2012;84:182–187. doi: 10.1016/j.ces.2012.08.029
[43] Remeli A, Nazar R, Ismail F, et al. Marangoni-driven boundary layer flow in a nanofluid with suction and injection. World Appl Sci J. 2012;17:21–26.
[44] Rashid U, Baleanu D, Liang H, et al. Marangoni boundary Layer flow and Heat Transfer of Graphene–water nanofluid with particle shape effects. Processes. 2020;8(9):1120. doi: 10.3390/pr8091120
[45] Khan NM, Chu YM, Khan MI, et al. Modeling and dual solutions for magnetized mixed convective stagnation point flow of upper convected Maxwell fluid model with second-order velocity slip. Math Meth Appl Sci. 2020;1–21. doi: 10.1002/mma.6824